*Article*

# Adaptive Modulation Scheme for Soft-Switching Hybrid FSO/RF Links Based on Machine Learning

**Junhu Shao [1], Yishuo Liu [1], Xuxiao Du [1] and Tianjiao Xie [2,*]**

[1] Xi'an Key Laboratory of Wireless Optical Communication and Network Research, School of Automation and Information Engineering, Xi'an University of Technology, Xi'an 710048, China; jhshao@xaut.edu.cn (J.S.)
[2] China Academy of Space Technology (Xi'an), Xi'an 710100, China
* Correspondence: xiexietianjiao@163.com

**Abstract:** A hybrid free-space optical (FSO) and radio frequency (RF) communication system has been considered an effective way to obtain a good trade-off between spectrum utilization efficiency and high-rate transmission. Utilizing artificial intelligence (AI) to deal with the switching and rate adaption problems between FSO/RF links, this paper investigated their modulation adapting mechanism based on a machine learning (ML) algorithm. Hybrid link budgets were estimated for different modulation types in various environments, particularly severe weather conditions. For the adaptive modulation (AM) scheme with different order PPM/PSK/QAM, a rate-compatible soft-switching model for hybrid FSO/RF links was established with a random forest algorithm based on ML. With a given target bit error rate, the model categorized a link budget threshold of the hybrid FSO/RF system over a training data set from local weather records. The switching and modulation adaption accuracy were tested over the testing weather data set especially focusing on rain and fog. Simulation results show that the proposed adaptive modulation scheme based on the random forest algorithm can have a good performance for soft-switching hybrid FSO/RF communication links.

**Keywords:** adaptive modulation; hybrid FSO/RF link; link budget; machine learning

## 1. Introduction

Free-space optical (FSO) communication, known as optical wireless communication (OWC), has the advantages of a license-free spectrum, large bandwidth, flexible network and high data rate. However, FSO links are inevitably affected by atmospheric turbulence and adverse meteorological situations, including snow, fog, dust, etc. Radio frequency (RF) communication can provide a reliable link but is sensitive to rainy circumstances, especially for microwave and millimeter wave systems. To address these vulnerabilities, the past decade has witnessed growing interest in the integration of FSO link and RF link, forming hybrid FSO/RF heterogeneous networks. Such amalgamated systems aim to capitalize on the complementary strengths of both communication technologies, thereby enabling more efficient and reliable data transmission [1–4].

There are two modes for using FSO/RF links: hard-switching and soft-switching. In soft switching mode, both links are active simultaneously [5,6]. Only one link is active in hard switching mode [7]. For mixed channels, a new throughput maximization algorithm was proposed in [5] to optimize the bit rate, and the system performance of LDPC codes with regular or irregular structures was analyzed. In [6], data were simultaneously transmitted over two links at the same rate, and space diversity technology was adopted to maximize spectrum utilization and reduce the influence of the turbulence channel. Through the analysis of outage probability, ref. [7] studied the performance of a hybrid FSO/intelligent reflecting surface (IRS)-aided RF communication system based on hard switching. Experimental results showed that the outage probability increases with the increase in the switching threshold, and the increase in the signal-to-noise power ratio

(SNR) suppressed outage performance. Additionally, deploying more elements in the IRS could result in SNR gain. When hard switching worked, ref. [8] used a machine learning (ML) algorithm to predict the indicator of received signal strength (RSSI), which proved the reliability of hard switching. RSSI considered the values of the current state and the previous state, and the proper selection of threshold limits for the RSSI parameter was crucial: when the RSSI exceeded the threshold, the FSO link was chosen, whereas when it fell below the threshold, the RF link was selected.

Several researchers have explored channel prediction based on ML algorithms, including hybrid links, especially those combined with adaptive modulation (AM). In [9], a proposal was made for a method of estimating SNR using artificial neural networks in AM and coding schemes. Power spectral density was used to classify SNR and played a role in adaptive coding and modulation. Once trained, it could determine the optimal adaptive coding and scheme at lower complexity, demonstrating its effectiveness in throughput performance. The possibility of using AM to select and switch modulation modes in hybrid link systems was proposed and verified by using intelligent power control and link switching in [10]. It demonstrated that not only could the variation trend in RSSI be predicted, but also that power control could effectively reduce switching frequency, thereby enhancing the transmission quality of FSO link. In [11], the ML algorithm was used to predict channel state information, in which the SNR of the next transmission channel was taken as the prediction target, and the past SNR with other relevant information was treated as the prediction basis. In [12], the ML model was used to train the amplitude-frequency vector of data symbols with the goal of matching the SNR and achieving SNR estimation. The experiment showed that even with very low SNR, ML could estimate the SNR with very high accuracy, even reducing the mean square error to less than 0.01. Ref. [13] proposed a hybrid FSO/RF system that manipulates adaptive switching techniques to form IM/DD and coherent heterodyne detection; finally, the expression of outage probability under various atmospheric conditions was obtained and was used as a criterion to compare single FSO systems with hybrid systems. Ref. [14] proposed a link-switching mechanism based on ML in a hybrid FSO/RF system, the system utilized ML to predict the link margin and achieve link prediction based on weather conditions. As far as we know, the issue of ML-based modulation switching and link threshold for hybrid links considering weather data has not been addressed. This work is based on link thresholds and uses ML to select modulation for communication links based on current atmospheric conditions.

The rest of this paper is organized as follows: Section 2 examines the proposed a hybrid FSO/RF model of an ML-based switching system and discusses the different atmospheric effects. Section 3 discusses the ML model in determining link availability, deriving expressions for its spectral efficiency, link budget (LB), and bit error rate (BER). Section 4 describes the simulation results, and useful concluding remarks are drawn in Section 5.

## 2. Hybrid FSO/RF Link System

Firstly, we present a ML-based soft-switching model for hybrid FSO/RF links, as shown in Figure 1. The model comprises transceivers for FSO/RF links that are connected to the switching system. FSO and RF channels are established simultaneously. The ML algorithm is used to calculate the LB, which defines the range of switching thresholds between the FSO and RF links under diverse modulation schemes. In this switching mechanism, the FSO link is designated as the primary communication channel, with the RF link assuming an auxiliary role.
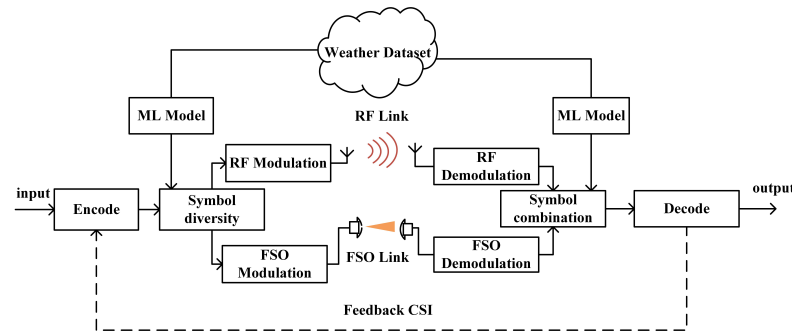
**Figure 1.** ML-based soft-switching model for Hybrid FSO/RF links.

### 2.1. Free Space Optical Channel

The received signal $r$ with the optical wireless system can be modeled as [15]

$$r = g_1 P \eta h_{FSO} x + n_1,$$ (1)

where $P$, $x$, and $\eta$ represent the average transmitted optical power, the transmitted signal, and the receiver's optical-to-electrical conversion efficiency, respectively. $h_{FSO}$ is the instantaneous optical channel intensity gain, $n_1$ is the additive white Gaussian noise, $g_1$ represents the specific attenuation resulting from the weather attenuation coefficient ($\alpha_1$), and their relationship is expressed as $g_1 = exp(-\alpha_1 L)$, and $L$ is the link distance. Assuming that $h_{FSO}$ obeys the gamma-gamma distribution, the instantaneous SNR is expressed as:

$$\gamma_{FSO} = \overline{\gamma}_{FSO} h_{FSO}^2,$$ (2)

where $\overline{\gamma}_{FSO}$ denotes the average SNR. The probability density function (PDF) of the FSO link due to the Gamma-Gamma fading model is [3]

$$f_{\gamma_{FSO}}(\gamma_{FSO}) = \frac{(\alpha\beta)^{\frac{\alpha+\beta}{2}}}{\Gamma(\alpha)\Gamma(\beta)\overline{\gamma}_{FSO}^{\frac{\alpha+\beta}{4}}} \gamma_{FSO}^{\frac{\alpha+\beta}{4}-1} K_{\alpha-\beta}\left(2\sqrt{\alpha\beta\sqrt{\frac{\gamma_{FSO}}{\overline{\gamma}_{FSO}}}}\right),$$ (3)

where $K_{\alpha-\beta}(.)$ represents the modified Bessel function of the second kind of order $\alpha - \beta$ and $\Gamma(.)$ denotes the Gamma function. $\beta$ and $\alpha$ given by [6] indicate the effective number of large-scale and small-scale eddies of the scattering process, respectively.

### 2.2. Radio Frequency Channel

The input signal $x_2$ undergoes upconversion to transform it into an RF signal prior to transmission. At the receiver's end, the signal undergoes demodulation, which can be described as

$$r_2 = \sqrt{P_2} h_{RF} x_2 + n_2,$$ (4)

where $n_2$ is the additive white Gaussian noise, $P_2$ and $h_{RF}$ indicate the average transmitted power and the channel fading coefficient of the RF link. Meanwhile, the RF link is modeled by the Rician distribution with the Rice parameter $K$, where $K$ represents the relative strength of the direct LOS path. The PDF of the RF fading is provided in [15]

$$f_{\gamma_{RF}}(\gamma_{RF}) = \frac{K+1}{\overline{\gamma}_{RF}} exp\left(-(K+1)\frac{\gamma_{RF}}{\overline{\gamma}_{RF}} - K\right) I_0\left(2\sqrt{K(K+1)\frac{\gamma_{RF}}{\overline{\gamma}_{RF}}}\right),$$ (5)

where $I_0(\cdot)$ is a zero-order modified Bessel function of the first kind, and $\gamma_{RF}$ represents the instantaneous SNR, which relates to $h_{RF}$ and average SNR $\overline{\gamma}_{RF}$ as $\gamma_{RF} = \overline{\gamma}_{RF} h_{RF}^2$.

*2.3. Atmospheric Attenuation for Hybrid Links*

Atmospheric attenuation signifies the reduction in signal power through the atmosphere, rendering it a crucial factor for consideration. Suppose the attenuation coefficient for the FSO link in foggy weather is $\alpha_{1,fog}$, which can be derived from Kim's model as [14]

$$\alpha_{1,fog} = \frac{3.91}{V(\text{km})} \left( \frac{\lambda(m)}{550 \times 10^{-9}} \right)^{-q} (\text{dB/km}), \tag{6}$$

where $V$ is the visibility, $\lambda$ is the wavelength, and the parameter $q$ varies with visibility as

$$q = \begin{cases} 1.6, & V > 50 \text{ km}, \\ 1.3, & 6 \text{ km} < V < 50 \text{ km}, \\ 0.16 \times V + 0.34, & 1 \text{ km} < V < 6 \text{ km}, \\ V - 0.5, & 0.5 \text{ km} < V < 1 \text{ km}, \\ 0, & V < 0.5 \text{ km}. \end{cases} \tag{7}$$

If the attenuation coefficient during rainfall is $\alpha_{1,rain}$, which is related to rain intensity $R$, the expression can be described as

$$\alpha_{1,rain} = 1.076 R^{0.67} (\text{dB/km}). \tag{8}$$

When the frequency of the RF link is below 10 GHz, the rain attenuation is calculated as follows [16]:

$$\alpha_{2,rain} = kR^{\alpha} (\text{dB/km}), \tag{9}$$

where the coefficients $k$ and $\alpha$ are the signal's frequency and the elevation angle. The attenuation of the RF link caused by fog can be expressed as

$$\alpha_{2,fog} = K_l M (\text{dB/km}), \tag{10}$$

where $M$ is the liquid water density in fog. $K_l$ is the specific attenuation coefficient.

## 3. Threshold Estimation and Data Set Generation by Machine Learning

According to the atmospheric characterization parameters given in the CCSDS141.1-R-1 red book, we gain the original data set $S_1$ from the website of https://rp5.ru/(accessed on 1 September 2020 to 1 December 2022), which involves rainfall rate, visibility, temperature, humidity, etc. The LB is used to plan the resource allocation for each modulation and to determine the working mode for hybrid FSO/RF links. The ML model is constructed to learn and predict from the data on rainfall and visibility on rainy and foggy days.

*3.1. Construction of the Random Forest Algorithm Model*

The random forest algorithm is an ensemble model suitable for classification problems, consisting of multiple decision trees. When training data are input into the model, a subset is randomly selected along with some of its feature attributes to build multiple small decision trees. When unknown data are input, predictions are made for each decision tree, and the final prediction is obtained through a voting process based on the predictions of the decision trees. In this experiment, 500 decision trees are selected, each with a maximum depth of 3.

The model works in two phases: the training part and the testing part. The training part includes defining the optimal range of multiple modulations based on a given target BER and $S_1$. Then, their corresponding LB threshold set $S_2$ can be calculated to allocate the channel state set $D_{i,i=1,2\cdots N}$. The FSO link has three modulation modes, including L-ary pulse-phase modulation (L-PPM), M-ary phase shift keying (M-PSK), and M-ary quadrature amplitude modulation (M-QAM). The RF link operates predominantly in two

modulation modes: M-PSK and M-QAM. In Algorithm 1, the details of calculating link budget by switching modulation is provided.

---

**Algorithm 1:** Link budget switching scheme

**Input:** $parameter_1$, $parameter_2$, $\cdots$, $parameter_n$ (1, 2, $\cdots$, n for modulation mode.)
**Result:** An optimum spanning random forest model, *LinkBudget*
**Data:** Weather set $S_1$
```
/* Now this is an if···else conditional loop                      */
```
1 for i = 1:length (rainfall rate (R) or visibility (V))
2 **if** *0 < R(i)/V(i) $\leq$ parameter$_1$* **then**
3 │  Modulation1;
4 **else if** *parameter$_1$ < R(i)/V(i) $\leq$ parameter$_2$* **then**
5 │  Modulation2;
6 ⋮ **else if** *parameter$_{n-1}$ < R(i)/V(i) $\leq$ parameter$_n$* **then**
7 │  Modulation*n*;
8 **else if** *R(i)/V(i) > parameter$_n$* **then**
9 │  Outage;
10 Substituting of *parameter$_1$*, *parameter$_2$*, $\cdots$, *parameter$_n$* into the formula of the *LinkBudget* results in $LB_1$, $LB_2$, $\cdots$, $LB_n$. Determine the total number of each modulation, along with the number of correct and incorrect judgments.

---

For the channel state of each modulation ($D_{i,i=1,2\cdots N}$) and the proper target BER ($P_{e,obj}$), set $S_1$ is taken into account to construct a relational graph that delineates the correlation between the weather parameter and the average BER ($\overline{P}_e$) across different modulations. The relational graph as shown in Figure 2 is divided into some areas representing the optimum modulation range when $\overline{P}_e$ is smaller than $P_{e,obj}$, and the $LB_{thi,i=1,2\cdots N}$ is calculated when $\overline{P}_e$ is equal to $P_{e,obj}$. And we calculate the LB from arbitrary weather data. A comparison between $LB$ and $LB_{thi,i=1,2\cdots N}$ determines the channel state ($S_2$). If it is less than the minimum threshold ($LB_{thi,min}$), the communication is interrupted. If it is between $LB_{thi}$ and $LB_{thi+1}$, the channel state of the current weather is $D_i$.
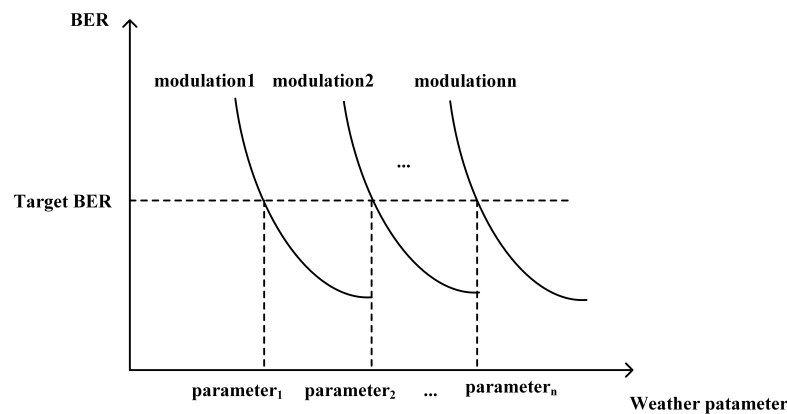


**Figure 2.** Optimum modulation range.

The second component focuses on constructing a random forest model that utilizes the weather set ($S_1$) and channel state set ($S_2$). Within the training phase, multiple channel states are formulated as the output labels for the decision trees. The optimal channel state can be obtained by inputting data from real-time weather into the random forest model, but it requires in-depth analysis to determine whether $\overline{P}_e$ of the channel state ($D_{i+1}$) under current weather data is less than $P_{e,obj}$. In cases where $\overline{P}_e$ exceeds $P_{e,obj}$, the LB threshold is

fine-tuned iteratively until it descends below $P_{e,obj}$. This iterative process is performed to produce the channel state congruent with the channel state set ($S_2$) established during the training phase.

*3.2. Basic Parameters*

3.2.1. Link Budget

LB refers to the remaining signal power or bandwidth in a communication link. Suppose $LB_{FSO}$ denotes the LB of the FSO link, and it can be expressed as [14]

$$LB_{FSO} = P_1 + |S_r| - \alpha_{FSO,atmo} - \alpha_{geo} - \alpha_{sys}, \tag{11}$$

where $P_1$ is the transmitter power, $S_r$ is the receiver sensitivity, $\alpha_{geo}$ is geometrical attenuation, $\alpha_{sys}$ is system losses, and the atmospheric attenuation in the FSO link is denoted as $\alpha_{FSO,atmo}$, which is a collective representation of $\alpha_{1,fog}$ and $\alpha_{1,rain}$. Suppose $LB_{RF}$ denotes the LB of the RF link, and it can be expressed as [11]

$$LB_{RF} = EIPR + G_r - \left(\frac{E_b}{N_0}\right)_{reg} - R - kT - L_s - \alpha_{RF,atmo}, \tag{12}$$

where $EIPR$ is the effective isotropic radiated power, $G_r$ indicates the receiver antenna gain, $\left(\frac{E_b}{N_0}\right)_{reg}$ represents the lowest normalized SNR, $R$ indicates the bit rate of the system, and $k$ is the Boltzmann constant. The receiver noise temperature is presented as $T$, $L_s$ represents path loss, and $\alpha_{RF,atmo}$ is the atmospheric attenuation under the RF link, given by $\alpha_{2,rain}$ and $\alpha_{2,fog}$.

3.2.2. Instantaneous BER

The average BER that reflects the performance of the system is the average value of the instantaneous BER over a time period. For the FSO link, the average BER ($\overline{P}_{b_1,modulation}$) can be given by the instantaneous BER ($P_{e,modulation}$) and the PDF, and is denoted as

$$\overline{P}_{b_1,modulation} = \int_0^\infty P_{e,modulation} f_{\gamma_{FSO}}(\gamma_{FSO}) d\gamma. \tag{13}$$

Similarly, the instantaneous BER of the RF link can be expressed as

$$\overline{P}_{b_2,modulation} = \int_0^\infty P_{e,modulation} f_{\gamma_{RF}}(\gamma_{RF}) d\gamma, \tag{14}$$

to express $\overline{P}_{b_2,modulation}$ as the average BER of the RF link. Simultaneously, the instantaneous BER of modulation modes can be expressed as

- BER of L-PPM:

$$P_{e,LPPM} = \frac{1}{2} erfc\left(\frac{\sqrt{\gamma \frac{L}{2} \log_2 L}}{2\sqrt{2}}\right), \tag{15}$$

  where L is the symbol order, $L = 2^n$.
- BER of M-PSK:

$$P_{e,BPSK} = \frac{1}{2} erfc(\sqrt{\gamma}), M = 2, \tag{16}$$

$$P_{e.MPSK} = \frac{1}{\log_2 M} erfc\left(\sin\frac{\pi}{M}\sqrt{\gamma}\right), M \geq 4, \tag{17}$$

  where M stands for the modulation length of PSK.

- BER of M-QAM: the instantaneous BER of M-QAM is shown as [17]

$$P_{e,MQAM} = \frac{2\left(\sqrt{M}-1\right)}{\sqrt{M}\log_2 M} erfc\left(\sqrt{\frac{3\log_2 M}{2(M-1)}\gamma}\right).$$ (18)

*3.3. Adaptive Modulation*

The spectral efficiency of M-PSK is defined as the data rate transmitted within a given bandwidth, and can be given by [18]

$$\eta_{MPSK} = \frac{C}{W} = \frac{\sum_{j=1}^{N} b_j \log_2 M_j}{2},$$ (19)

where $C$ represents the data rate used for transmission, $W$ shows the channel bandwidth, the modulation order is represented as $M_j$, $M_j = 2^j$, $j = 1, 2 \cdots N$, and $b_j$ is the probability of receiving SNR in the interval $[\gamma_j, \gamma_{j+1}]$, which can be expressed as

$$b_j = Pr\{\gamma_j \le \gamma_{j+1}\} = F_\gamma(\gamma_{j+1}) - F_\gamma(\gamma_j),$$ (20)

where $F_\gamma(.)$ is the cumulative distribution function (CDF) of the turbulence-induced fading. Given $F_\gamma(\gamma_{j+1}) \to 1$, (18) can be simplified to

$$\eta_{MPSK} = \frac{N - \sum_{j=1}^{N} F_\gamma(\gamma_j)}{2}.$$ (21)

And the spectral efficiency of the M-QAM is as follows [19]:

$$\eta_{MQAM} = \sum_{j=1}^{N} ja_j = N - \sum_{j=1}^{N} F(\gamma_j),$$ (22)

The spectral efficiency of the L-PPM is as follows [20], there is only one optical pulse among the N times slots:

$$\eta_{LPPM} = \frac{\log_2 L}{L}.$$ (23)

where have only one optical pulse among the $L$ times slots.

**4. Numerical Results**

*4.1. BER versus Link Budget*

The characterization of both the FSO link and RF link was substantiated through numerical simulations, and the specific parameters utilized for the simulation were detailed in Table 1. The comparison that obtains the relationship between weather and BER among the modulations is presented in Figures 3 and 4. The BER increases with worsening weather conditions. It is worth noting that the BER remains relatively stable on foggy days due to the strength of the RF link against fog.

Tables 2 and 3 show the LB thresholds for the modulations we have listed, indicating that the modulation order changes in adverse weather conditions. To achieve the switching of multiple modulations between the FSO link and RF link under rainfall rate and visibility changes, the target BER $P_{e,obj}$ needs to be set. The BER of these modulations should be lower than or equal to the set target BER $P_{e,obj}$. In the rain, $P_{e,obj}$ set on the FSO link is $10^{-6}$ and its value set on the RF link is $10^{-3}$. In the fog, $P_{e,obj}$ is set on the FSO link as $10^{-9}$. Given that the RF link has less variation on foggy days when using the random forest model, its $P_{e,obj}$ and threshold range are ignored.

**Table 1.** Parameters for Simulation.

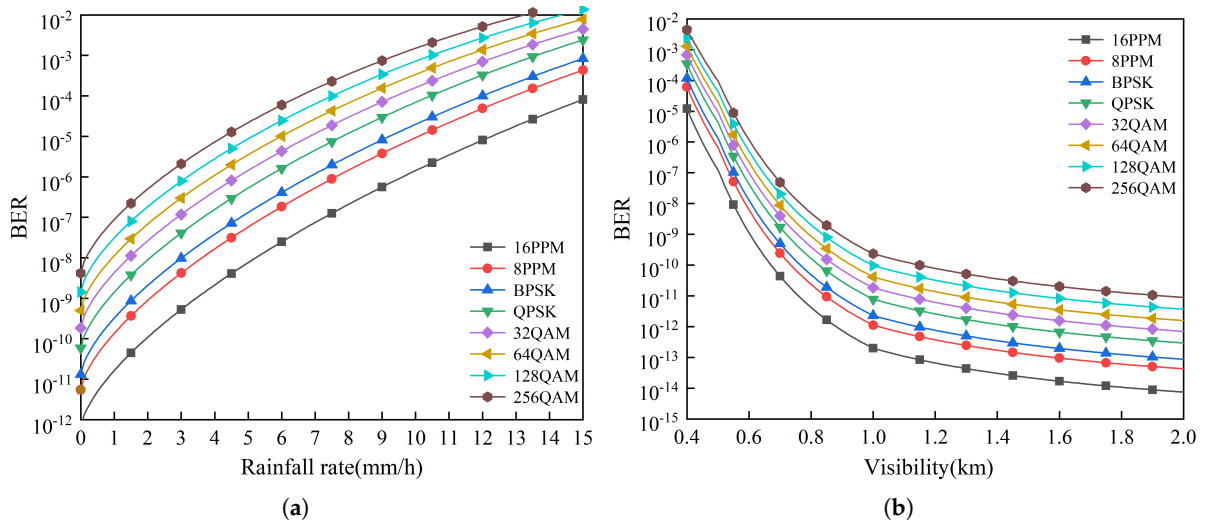| Parameter of FSO Sub-System | Value |
| --- | --- |
| Link range | 3 km |
| Wavelength | 1550 nm |
| Transmitting power | 50 dBm |
| System loss | 3 dB |
| Divergence angle | 1.25 mrad |
| Receiver sensitivity | −31 dBm |
| **Parameter of RF Sub-system** | **Value** |
| Link range | 3 km |
| Carrier frequency | 60 GHz |
| Receiver antenna gain | 44 dBi |
| Transmitting power | 40 dBm |
| Signal-to-noise power ratio | 50 dB |
| Bit rate | 84.1 bps |



(a)

(b)

**Figure 3.** Bit error rate performance of FSO system in rainy and foggy weather condition. (**a**) Rainfall rate. (**b**) Visibility.
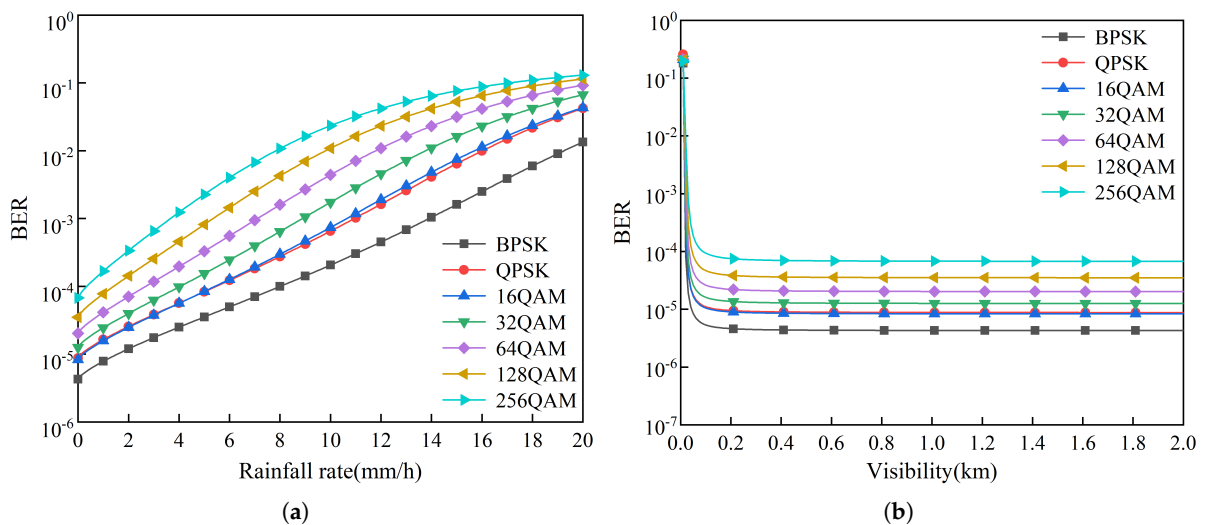


(a)

(b)

**Figure 4.** Bit error rate performance of RF system in rainy and foggy weather condition. (**a**) Rainfall rate. (**b**) Visibility.

**Table 2.** The range of LB threshold of FSO link.

| Modulation | FSO-Rain | FSO-Fog |
|---|---|---|
| Interrupt | $\leq$38.158 | $\leq$34.914 |
| 16PPM | 38.158~40.424 | 34.914~37.091 |
| 8PPM | 40.424~41.227 | 37.091~37.860 |
| BPSK | 41.227~42.798 | 37.860~39.249 |
| QPSK | 42.798~43.829 | 39.249~40.178 |
| 32QAM | 43.829~45.068 | 40.178~41.795 |
| 64QAM | 45.068~45.801 | 41.795~42.722 |
| 128QAM | 45.801~47.065 | 42.722~43.929 |
| 256QAM | $\geq$47.065 | $\geq$43.929 |

**Table 3.** The range of LB threshold of RF link.

| Modulation | RF-Rain |
|---|---|
| Interrupt | $\leq$35.313 |
| BPSK | 35.313~38.091 |
| QPSK | 38.091~38.517 |
| 16QAM | 38.517~40.378 |
| 32QAM | 40.378~42.456 |
| 64QAM | 42.456~44.554 |
| 128QAM | 44.554~46.849 |
| 256QAM | $\geq$46.849 |

*4.2. Comparison of the Prediction Model with the Real Modulation Selection*

The model is trained with 80% of the data and tested for the remaining 20%. A predefined threshold of 12.05 dB is used to classify the link. The test and training sets required for the model are selected randomly from the original data to ensure that the features and patterns learned by the model on the training set can be generalized to unseen data. Figures 5–7 all indicate the results from training and testing. The modulation order decreases as the rainfall rate increases and increases as the visibility increases. However, random forests contain randomness that can lead to varied results each time they are run. Incomplete modulation may be generated if the weather values during testing do not cover the entire range of the set weather values, as shown in Figure 6.

The case of the RF link in rainy conditions, as well as the FSO link in rainy and foggy conditions all have the same number of data points. Take the results of the FSO link in rainy conditions as an example. The total number of samples is 1346, the number of training sets is 1014, and the number of test sets is 332. Table 4 summarizes twice the results of the test set: 'Right' indicates the number of correct judgments, and 'Wrong' indicates the number of incorrect judgments. The first and second experiments are indicated by 1 and 2. The model compares the predicted results with the numerical labels in the test set and considers the prediction to be correct if they are consistent.

**Table 4.** The correctness rate of test sets from FSO link.

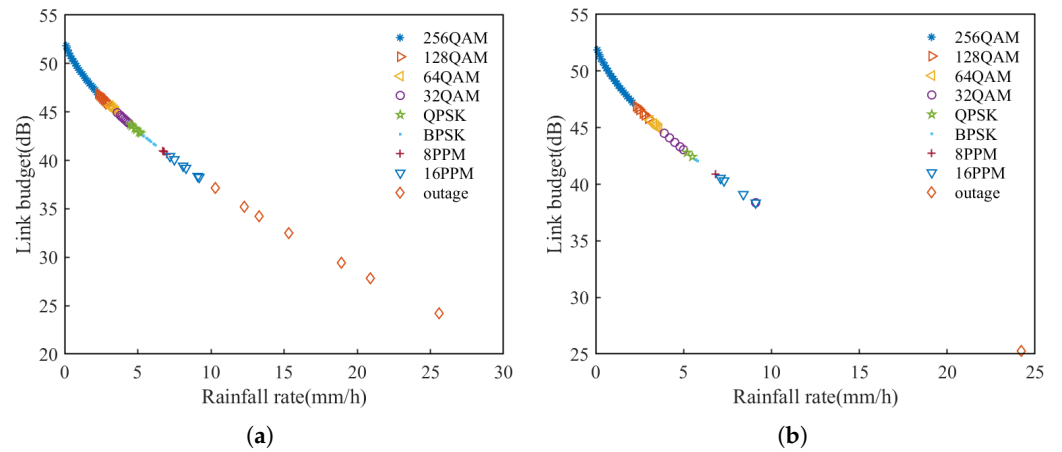| Modulation | Right 1 | Wrong 1 | Accuracy 1 | Right 2 | Wrong 2 | Accuracy 2 |
|---|---|---|---|---|---|---|
| 16PPM | 3 | 1 | 75.0% | 2 | 0 | 100.0% |
| 8PPM | 1 | 0 | 100.0% | 1 | 0 | 100.0% |
| BPSK | 4 | 2 | 66.7% | 2 | 0 | 100.0% |
| QPSK | 1 | 3 | 25.0% | 5 | 1 | 83.4% |
| 32QAM | 7 | 0 | 100.0% | 7 | 2 | 77.8% |
| 64QAM | 3 | 1 | 75.0% | 5 | 0 | 100% |
| 128QAM | 10 | 1 | 90.9% | 9 | 2 | 81.8% |
| 256QAM | 292 | 0 | 100.0% | 293 | 0 | 100% |
| Outage | 1 | 2 | 33.3% | 2 | 1 | 66.7% |

**Figure 5.** Classification of modulations for FSO link in rainy weather. (**a**) Results of training set. (**b**) Results of test set.
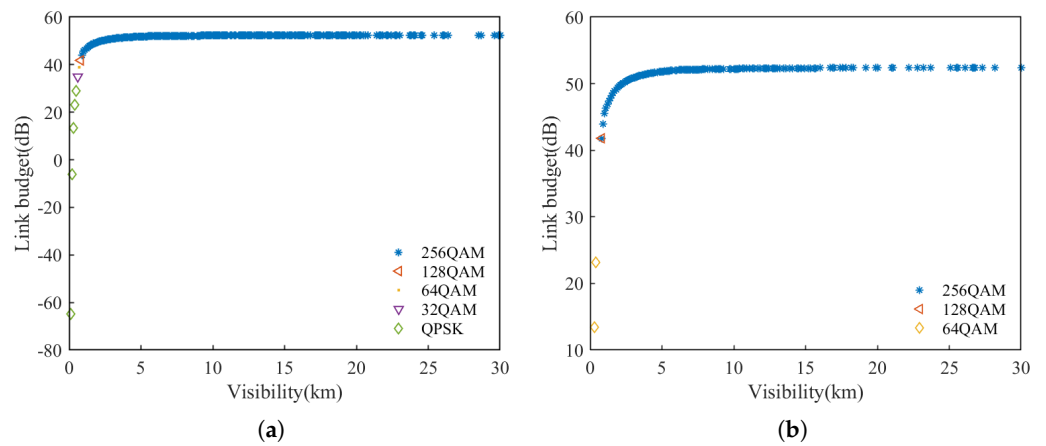


**Figure 6.** Prediction of modulations for FSO link in foggy weather. (**a**) Results of training set. (**b**) Results of test set.
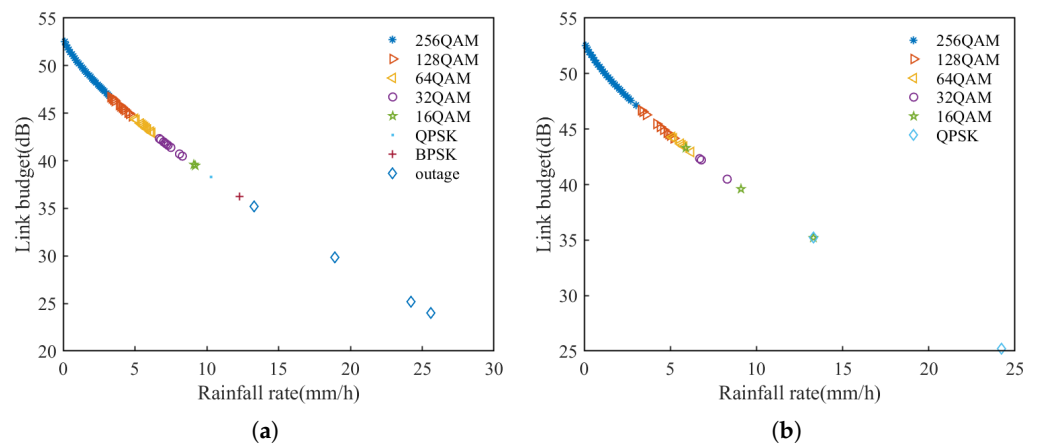


**Figure 7.** Classification of modulations for RF link in rainy weather. (**a**) Results of training set. (**b**) Results of test set.

### 4.3. The Impact of Decision Trees on Performance in Random Forests Algorithm

The final prediction result of the random forest is obtained by combining the results of all decision trees. Each decision tree outputs a classification label, and the model determines the final classification result by majority voting on the classification labels output by all

decision trees. In Figure 8, the relationship between the number of decision trees and accuracy is displayed. The experiment simulated the results from 50 trees to 1000 trees with a step of 50, each tree being run 100 times. In this experiment, a total of 500 decision trees were used, corresponding to an accuracy of 0.997 for FSO links in foggy conditions. In rainy conditions, the accuracy of the RF link is 0.989, and the FSO link accuracy is 0.975.
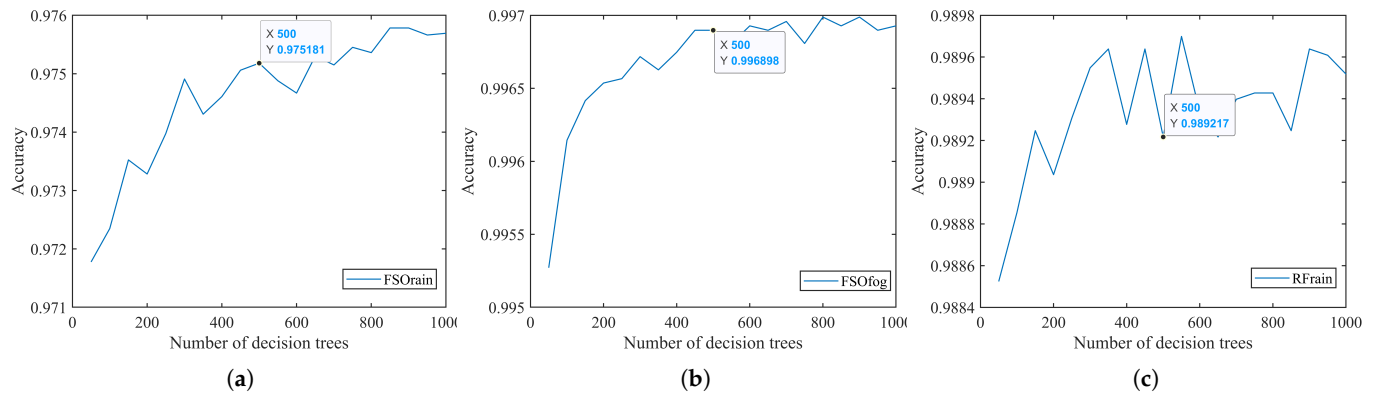


**Figure 8.** The relationship between decision trees and classification accuracy. (**a**) Accuracy of FSO link in rain. (**b**) Accuracy of FSO link in fog. (**c**) Accuracy of RF link in rain.

In each decision tree, the feature selection at each node is random, and not all features are used for training. This random feature selection makes the rules of the decision tree more randomized, helping to prevent overfitting and improving the accuracy and stability of the data.

## 5. Discussion

This paper uses a machine learning-based random forest algorithm to implement a soft-switching strategy in hybrid FSO/RF links and evaluate their performance. The random forest model is established according to the channel parameters, particularly focusing on rain and fog as the primary elements. Because the performance of the hybrid link is limited by severe weather conditions. With a weather data set split into a training part and a test part, the modulation adaptation accuracy performance was simulated. The results show that the training results of each group are consistent with the homologous testing results. The AI-based soft-switching strategy can enhance communication quality and reliability according to real-time environmental weather conditions. Furthermore, by using the trained link budget threshold, a suitable modulation type can be chosen to maximize the system efficiency with double links.

Compared to [14], this work incorporates considerations for modulation. When determining the link quality model, real-time rain and fog data are used for training, in addition to taking into account the target BER. In order to align with the modulation, the LB is divided to ensure the stability and reliability of link performance. In order to maintain a balance in accuracy, this alignment may lead to a slight decrease in accuracy. Subsequently, we will continue to research this task, striving to achieve 100% prediction accuracy by conducting experimental testing with more external factors taken into account in some practical application scenarios. This will provide strong support for high-speed data transmission.

**Author Contributions:** Conceptualization, J.S. and X.D.; methodology, J.S., Y.L., X.D. and T.X.; software, J.S.; validation, Y.L., X.D. and T.X.; formal analysis, X.D.; investigation, J.S., Y.L., X.D. and T.X.; data curation, Y.L. and X.D.; writing—original draft preparation, J.S., Y.L., X.D. and T.X.; writing—review and editing, J.S., Y.L. and X.D.; visualization, J.S.; supervision, J.S. and T.X. All authors have read and agreed to the published version of the manuscript.

**Institutional Review Board Statement:** Not applicable.

**Informed Consent Statement:** Not applicable.

**Data Availability Statement:** Data is contained within the article.

**Conflicts of Interest:** The authors declare no conflicts of interest.

## Abbreviations

The following abbreviations are used in this manuscript:

| | |
|---|---|
| FSO | Free space optical |
| RF | Radio frequency |
| AM | Adaptive modulation |
| ML | Machine learning |
| LB | Link budget |
| OWC | Optical wireless communication |
| SNR | Signal-to-noise power ratio |
| PDF | Probability density function |
| BER | bit error rate |
| L-PPM | L-ary pulse-phase modulation |
| M-PSK | M-ary phase shift keying |
| M-QAM | M-ary quadrature amplitude modulation |
| CDF | Cumulative distribution function |

## References

1. Mohsan, S.A.H.; Khan, M.A.; Amjad, H. Hybrid FSO/RF networks: A review of practical constraints, applications and challenges. *Opt. Switch. Netw.* **2023**, *47*, 100697. [CrossRef]
2. Kiran, K.V.; Rathore, S.; Turuk, A.K.; Das, S.K. Development of a Hybrid FSO/RF System during Link Misalignment. In Proceedings of the 2017 International Conference on Networking and Network Applications (NaNA), Kathmandu, Nepal, 16–19 October 2017; pp. 138–140. [Crossref]
3. Nath, S.; Shrivastava, S.K.; Sengar, S.; Singh, S.P. Novel Architectures for Efficient RF Usage in Hybrid FSO/RF System. In Proceedings of the 2018 IEEE International Conference on Advanced Networks and Telecommunications Systems (ANTS), Indore, India, 16–19 December 2018; pp. 1–6. [CrossRef]
4. Alathwary, W.A.; Altubaishi, E.S. On the Performance Analysis of Decode-and-Forward Multi-Hop Hybrid FSO/RF Systems With Hard-Switching Configuration. *IEEE Photon. J.* **2019**, *11*, 7907012. [CrossRef]
5. Khan, M.N.; Gilani, S.O.; Jamil, M.; Rafay, A.; Awais, Q.; Khawaja, B.A.; Uzair, M.; Malik, A.W. Maximizing Throughput of Hybrid FSO-RF Communication System: An Algorithm. *IEEE Access* **2018**, *6*, 30039–30048. [CrossRef]
6. Shakir, W.M.R. Performance Evaluation of a Selection Combining Scheme for the Hybrid FSO/RF System. *IEEE Photon. J.* **2018**, *10*, 7901110. [CrossRef]
7. Mondal, S.; Bhowal, A.; Kashyap, S.; Singh Kshetrimayum, R.; Patra, M. Outage probability analysis of hard-switching based mixed FSO/IRS-aided RF communication. In Proceedings of the 2023 National Conference on Communications (NCC), Guwahati, India, 23–26 February 2023; pp. 1–6. [Crossref]
8. Lapčak, M.; Ovseník, L.; Oravec, J.; Zdravecký, N. Design of hard switching for FSO/RF hybrid system based on prediction of RSSI parameter and environmental conditions. In Proceedings of the 2022 32nd International Conference Radioelektronika (RADIOELEKTRONIKA), Kosice, Slovakia, 21–22 April 2022; pp. 1–6. [Crossref]
9. Kojima, S.; Maruta, K.; Ahn, C.-J. Adaptive Modulation and Coding Using Neural Network Based SNR Estimation. *IEEE Access* **2019**, *7*, 183545–183553. [CrossRef]
10. Song, S.; Liu, Y.; Xu, T.; Guo, L. Hybrid FSO/RF System Using Intelligent Power Control and Link Switching. *IEEE Photon. Technol. Lett.* **2021**, *33*, 1018–1021. [CrossRef]
11. Wang, X.; Li, H.; Wu, Q. Optimizing Adaptive Coding and Modulation for Satellite Network with ML-based CSI Prediction. In Proceedings of the 2019 IEEE Wireless Communications and Networking Conference (WCNC), Marrakesh, Morocco, 15–18 April 2019; pp. 1–6. [Crossref]
12. Ahn, J.-Y.; Wang, H. Machine Learning-based Signal-to-Noise Ratio Estimation using Amplitude Frequency Vector. In Proceedings of the 2023 International Conference on Electronics, Information, and Communication (ICEIC), Singapore, 5–8 February 2023; pp. 1–3. [Crossref]
13. Gupta, A.; Chauhan, K.; Yadav, A.; Rani, R.; Jain, A.; M, L. Performance Analysis of Adaptive Combining Based Hybrid FSO/RF Communication System with Pointing Errors Over F-Distribution/ Nakagami-m Channel Models. In Proceedings of the 2023 2nd International Conference on Vision Towards Emerging Trends in Communication and Networking Technologies (ViTECoN), Vellore, India, 5–6 May 2023; pp. 1–7. [Crossref]

14. Kiran, K.V.; Perinbaraj, S.; Pradhan, J.; Mallick, P.K.; Turuk, A.K.; Das, S.K. Machine Learning Aided Switching Scheme for Hybrid FSO/RF Transmission. *Intell. Decis. Technol.* **2021**, *14*, 529–536. [CrossRef]

15. Touati, A.; Abdaoui, A.; Touati, F.; Uysal, M.; Bouallegue, A. On the effects of combined atmospheric fading and misalignment on the hybrid FSO/RF transmission. *J. Opt. Commun. Netw.* **2016**, *8*, 715–725. [CrossRef]

16. Sudhakar, K.; Subramanyam, M.V. Evaluation of atmospheric attenuation due to various parameters. In Proceedings of the 2013 International Conference on Information Communication and Embedded Systems (ICICES), Chennai, India, 21–22 February 2013; pp. 609–612. [Crossref]

17. Lu, D.; Zhou, X.; Yang, Y.; Huo, J.; Yuan, J.; Long, K.; Yu, C.; Lau, A.P.T.; Lu, C. Theoretical analysis of PAM-N and M-QAM BER computation with single-sideband signal. *Sci. China Inf. Sci.* **2021**, *64*, 182312. [CrossRef]

18. Chatzidiamantis, N.D.; Lioumpas, A.S.; Karagiannidis, G.K.; Arnon, S. Adaptive Subcarrier PSK Intensity Modulation in Free Space Optical Systems. *IEEE Trans. Commun.* **2011**, *59*, 1368–1377. [CrossRef]

19. Afridi, S.; Hassan, S.A. Spectrally efficient adaptive generalized spatial modulation MIMO systems. In Proceedings of the 2017 14th IEEE Annual Consumer Communications Networking Conference (CCNC), Las Vegas, NV, USA, 8–11 January 2017; pp. 260–263. [Crossref]

20. Zhou, Z.; Liang, B.; Cao, Y.; Zhang, M. MPPM Spectrum Analysis Based on PPM. In Proceedings of the 2022 14th International Conference on Computer Research and Development (ICCRD), Shenzhen, China, 7–9 January 2022; pp. 356–362. [Crossref]